

# Circular Dichroism and Isotropy – Polarity Reversal of Ellipticity in Molecular Films of 1,1'-Bi-2-Naphthol

Alexander von Weber,<sup>[a]</sup> David C. Hooper,<sup>[b, c]</sup> Matthias Jakob,<sup>[a]</sup> Ventsislav K. Valev,<sup>[b, c]</sup> Aras Kartouzian,<sup>\*[a]</sup> and Ueli Heiz<sup>[a]</sup>

We have studied the circular dichroism (CD), in the ultraviolet and visible regions, of the transparent, chiral molecule 1,1'-Bi-2-naphthol (BINOL) in 1.5  $\mu\text{m}$  thick films. The initial transparent film shows an additional negative cotton effect in the CD compared to solution. With time under room temperature the film undergoes a structural phase transition. This goes hand in hand with a cotton effect at the low energy absorption band which inverts with opposite propagation direction of light through the film which is revealed as a polarity reversal of ellipticity (PRE). After completion of the phase transition the film exhibits

circular differential scattering throughout the visible range which also shows PRE. The structure change was studied with Raman, microscopy under cross polarization conditions and nonlinear second-harmonic generation circular dichroism (SHG-CD). The superposition of the optical activity of individual molecules and isotropy effects makes an interpretation challenging. Yet overcoming this challenge by finding a suitable model structural information can be derived from CD measurements.

## 1. Introduction

If light travels through optically active media, its linearly polarized plane rotates, which is called optical rotatory dispersion (ORD). This is described by a difference between the real parts of the indices of refraction for left-/right-handed circularly polarized light. In an adsorptive, chiral medium this is accompanied by a difference in absorption of left and right circularly polarized light, which is known as circular dichroism (CD).<sup>[1]</sup> The optical activity is caused by chiral molecules within the medium and additionally it can also originate from structural properties. This superposition makes an interpretation more challenging in comparison to solution. However, if the individual contributions can be assigned and understood, additional information about the structure can be derived. Within this work, correlations between optical activity and structural properties are studied to bring further insight to this topic.

One effect related to structural properties is called polarity reversal of ellipticity (PRE). It describes the inversion in sign of the optical activity when light propagates in the opposite direction through the medium. This antisymmetric behavior breaks time reversal symmetry and the Lorentz reciprocity and

is commonly known from magneto-optical effects like the Faraday effect. There an external magnetic field results in a magnetization direction within the medium which determines the ellipticity.

Recently metamaterials were presented where PRE was observed through enantiomerically sensitive plasmonic excitations in the absence of an external magnetic field and described as asymmetric transmission.<sup>[2]</sup> PRE was also studied in chiral double-layer meta-interfaces of chiral, transparent molecules and nonchiral, absorptive molecules. The effect was explained by a virtual magnetic field connected to a different index of refraction for both propagation directions.<sup>[3]</sup>

Within this work two independent PRE effects of enantiopure 1,1'-Bi-2-naphthol (BINOL) films are observed. BINOL consists of two 2-naphthol units connected through a C–C bond. The planes of the two 2-naphthol units are angled towards each other resulting in an overall axial chirality, see Figure 1. BINOL and its derivatives possess a high relevance as chiral ligands and modifiers and was therefore chosen as a model molecule.<sup>[4,5]</sup> The system neither possesses a meta-interface nor a plasmonic character and therefore presents an alternative material exhibiting PRE. The effects' nature as well as the connected film structure is investigated.

## Experimental Section

The samples were prepared by evaporation of enantiopure (R)-/(S)-BINOL on BK7 substrates or on silicon wafer with an artificial oxide layer in the case of the SHG-CD and cross polarization measurement. The 150  $\mu\text{m}$  thick substrates were cleaned with spectroscopic clean acetone and then sputtered with  $\text{Ar}^+$  under ultra-high vacuum (UHV) conditions. Afterwards the BINOL was evaporated on the glass substrate under high vacuum conditions. The substrate was kept at room temperature during the evaporation and the

[a] A. von Weber, M. Jakob, Dr. A. Kartouzian, Prof. U. Heiz  
Chair of Physical Chemistry, Chemistry Department & Catalysis Research  
Center, Technical University of Munich, Lichtenbergstr. 4, D-85748 Garching,  
Germany  
E-mail: aras.kartouzian@mytum.de

[b] D. C. Hooper, Dr. V. K. Valev  
Centre for Photonics and Photonic Materials, Department of Physics, Uni-  
versity of Bath, Claverton Down, Bath, BA2 7AY, United Kingdom

[c] D. C. Hooper, Dr. V. K. Valev  
Centre for Nanoscience and Nanotechnology, Department of Physics, Uni-  
versity of Bath, Claverton Down, Bath, BA2 7AY, United Kingdom

Supporting information for this article is available on the WWW under  
<https://doi.org/10.1002/cphc.201800950>

experiments. The details of the used vacuum setup are described elsewhere.<sup>[6]</sup>

A J-815 CD-spectrometer was used to acquire the extinction and CD spectra between 300 nm and 500 nm with the sample surface plane perpendicular to the light path. The spectra were taken in two geometries. In the first, light enters the BINOL film and then the glass substrate. Which is referred to as "R/S-BINOL  $\triangleright$  BK7". In the second case the sample is flipped 180° and light hits the glass first which is labeled as "BK7  $\triangleright$  R/S-BINOL". For a better understanding the geometric configuration is sketched in Figure 1. It was taken care that the same circular region with a diameter of ca. 13 mm of the sample was probed in both directions.

The SHG-CD experiments were done in reflection mode with a 45° angle of incidence. Left and right circularly polarized light of a fs laser system at 800 nm was focused on the sample while the sample was rotated around the surface normal. Light intensity of the second harmonic (SH) with a wavelength of 400 nm, which was generated at the sample, was detected by a photomultiplier tube. A detailed description of the setup is given elsewhere.<sup>[7]</sup>

Raman spectra were obtained with an inVia Qontor Raman microscope from Renishaw where an excitation wavelength of 633 nm was chosen.

Darkfield and cross polarization measurements were carried out with a Zeiss Axio Imager M2 microscope and additional absorption measurements in diffusive transmittance with a Lambda 650 spectrophotometer from BerkinElmer equipped with an Ulbricht sphere.

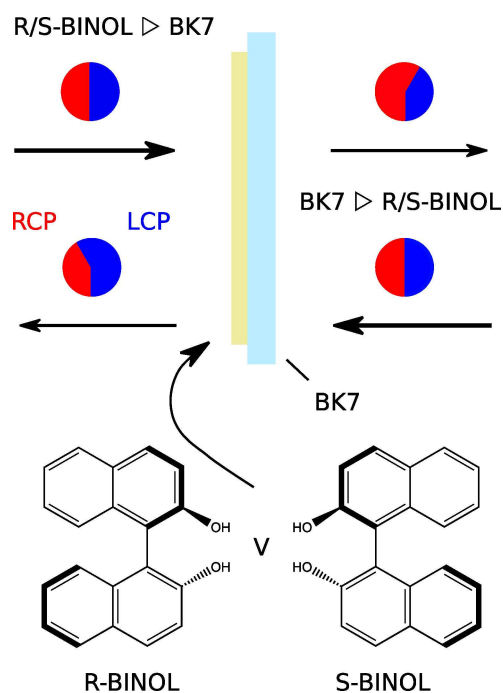


**Figure 1.** Experimental geometry including label for both light propagation direction configurations.

## 2. Results and Discussion

### 2.1. Linear Optical Activity

As a starting point and for comparison the extinction and CD of R-BINOL dissolved in ethanol were measured and are shown in Figure 2a. The extinction shows the low energy band (LEB) of

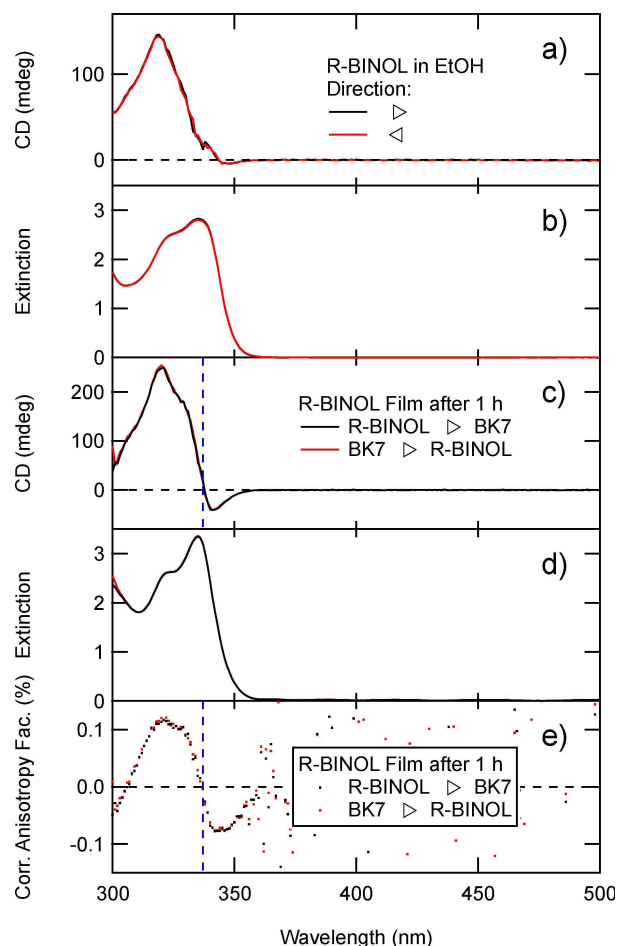


**Figure 2.** CD (a) and extinction (b) spectrum for both propagation directions of R-BINOL in EtOH and as film 1 h after evaporation (c), (d). Difference in anisotropy factor (e).

the long-axis polarization of both naphthol molecules as building block of BINOL. Due to coupling of the excited states of both naphthols an exciton-split state is formed resulting in two transitions from a common ground state.<sup>[8,9]</sup> This low energy band shows a positive band in the CD spectrum for the R enantiomer. Above ca. 360 nm the solution is fully transparent and shows no extinction nor optical activity. Both extinction and CD are invariant under sample rotation. The extinction and CD spectra of both enantiomers at smaller wavelength in solution is shown in Figure S1. A comparison to previously reported spectra proves their optical purity.<sup>[10]</sup>

Immediately after the evaporation the samples were taken out of the UHV system. They were fully transparent by eye (see

Figure S2a). The extinction and CD were measured 1 h after the evaporation for the first time and are shown in Figure 2b. The extinction shows the known LEB with a positive band in the CD spectrum and no activity above 360 nm. Additionally, the CD spectrum shows a negative feature at the flank of the band in the range between 325 nm and 360 nm. To isolate the effect the anisotropy factor of the solution is subtracted from one of the evaporated samples (Figure 2c). The anisotropy factor is equal the difference in absorption between left and right handed circularly polarized light weighted with the absorption resulting in a dimensionless quantity which is independent of concentration.<sup>[1]</sup> It reveals that this feature is a negative cotton effect with its crossing point at 337 nm. Again, the extinction and the CD of the initial, transparent film are invariant under sample rotation.

The film thickness was estimated to be 1.5  $\mu\text{m}$  based on the interference pattern in the extinction spectrum (Figure S3) near the absorption edge and independently the measured loading on a quartz crystal microbalance (Figure S4).

Several effects are likely to cause the difference in optical activity between solution and film, appearing as cotton effect in the latter case. First, a solvent effect that is absent in the film. Second, an interaction between neighboring molecules in the means of e.g. dipole-dipole interactions. Third, the dihedral angle between the naphthol monomers is different and known to influence the optical activity.<sup>[11]</sup> In solution it is about  $90^\circ$ .<sup>[12]</sup> In crystalline form depending on the crystal structure, it can adopt values between  $68.6^\circ$ <sup>[13]</sup> (racemic, flat, diamond shaped) and  $103.1^\circ$ <sup>[14]</sup> (chiral, tetragonal bipyramidal). Because the films were prepared from enantiopure BINOL, only the latter would be possible.

After 6 hours at room temperature small white spots were visible by eye in the film (see Figure S2b). The appearance of white spots is an indication of a restructuring within the film beginning from multiple seeds. The extinction and the CD at this state is given in Figure 3a. Compared to the 1 h old sample the extinction has not changed. However, the CD spectrum shows a new feature in the region of the absorption bands flank between 335 nm and 360 nm. To focus on this effect, the CD of the 1 h old sample is subtracted (Figure 3b) and smoothed curves are shown as solid line. The difference in CD shows a negative cotton effect with an asymmetry in width and magnitude left and right from the crossing point at 340 nm in the "R/S-BINOL  $\triangleright$  BK7" geometry. While the body of the CD band stays invariant under sample rotation the feature changes into a positive cotton effect when the light first hits the glass, i.e. PRE.

The appearance is unambiguously connected to a restructuring within the film. Decomposition or other effects can be excluded because both absorption and CD were unchanged except the new feature and furthermore BINOL is known to be stable in air and at room temperature. Therefore, the new feature at 340 nm is likely related to the observed beginning of a restructuring. In the course of such a structural change the molecules are reorientating in general and especially also towards each other. Accordingly, it is proposed that the effect is caused by interactions between neighboring molecules via

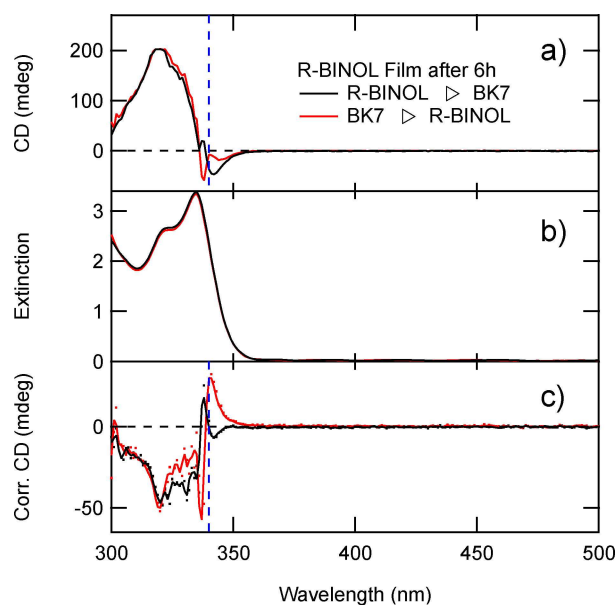


**Figure 3.** CD (a) and extinction (b) spectrum for both propagation directions of R-BINOL film 6 h after evaporation and difference in CD between 6 h and 1 h (c).

dipole-dipole interactions. This cotton effect has also been observed in vitrified liquid crystalline films of chiral polyfluorene.<sup>[15]</sup> But it has not been investigated in the sense of PRE but circular differential scattering which will also play a role later. Compared to the above-mentioned systems, which showed PRE the system presented here does not possess a double-layer meta-interface nor an enantiomerically sensitive plasmon. We do not have any different explanation for it. We believe therefore that PRE is not limited to such systems. In contrast the optical activity of the main CD band is a property of individual molecules and consequently not influenced by propagation direction of the light through the sample.

When left for 3 days the samples looked milky, white by eye (see Figure S2c). The structure of the LEB changed including a new peak at 328 nm (Figure 4a). Additionally, the film showed extinction at higher wavelengths throughout the visible range. The structure of the CD band at the low energy absorption band changed too. The previous observed feature at 340 nm increased in intensity and the sample showed optical activity throughout the whole range including the visible range where it was inactive before. The optical activity underwent PRE under sample rotation in the visible range as well as the previous described feature at 340 nm whereas the optical activity at wavelengths of the LEB are offset.

A film of the opposite *S* enantiomer shows the same extinction as anticipated (Figure 4b). The structure of the CD band at the LEB is similar but opposite in sign as expected for normal systems. However, the feature at 340 nm is reversed comparing the same direction and inverts under sample rotation as seen before. In contrast, the optical activity in the visible range does not change in sign with change of the

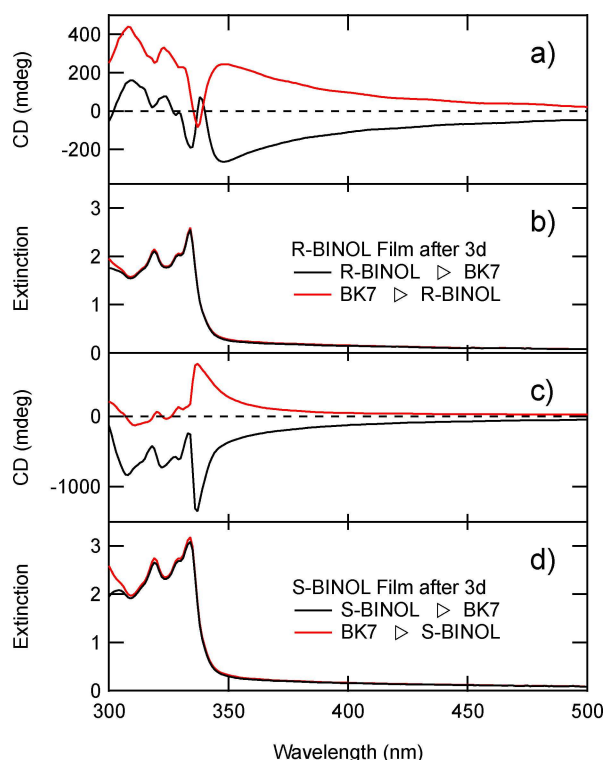


**Figure 4.** CD (a) and extinction (b) spectrum for both propagation directions of R-BINOL film and S-BINOL (c),(d) 3 d after evaporation.

enantiomer but again reverses in the opposite sample alignment.

By the appearance of the sample the restructuring process went on and seemed completed at this point by an overall milky, white appearance. The fact that the feature at 340 nm simultaneously increased in optical activity with the ongoing restructuring affirms the proposed connection. Another question is whether the measured extinction in the visible range is indeed absorption or scattering, which cannot be distinguished with the CD spectrometer. If the onset in extinction in this region is fitted with a power function, an inverse dependency of the order of 4 on the wavelength is evaluated (Table S1 and Figure S5). This is the dependency of Rayleigh scattering. To prove this point further an absorption spectrum of the R-BINOL film was measured in diffusive transmittance mode in a spectrophotometer equipped with an Ulbricht sphere where clearly only absorption is detected (Figure S6). The spectrum shows no absorption in the visible range and is qualitatively comparable to the 1 h and 6 h old film. This is final evidence that the film does not absorb in the visible region but scatters. Consequently, the optical activity in the visible region is a circular differential scattering phenomenon<sup>[16]</sup> and related to the macroscopic structure of the film and not the molecules itself. The clear dominance of scattering also rules out circular differential reflection as mechanism which has been concluded in case of differential scattering of vitrified liquid crystalline films of chiral polyfluorene too.<sup>[15]</sup> That the macroscopic structure and not individual molecules are related to the

circular differential scattering is supported by the fact that the sign of the optical activity at these wavelengths is independent of the enantiomer but alters with the direction of light through the sample.

A similar prepared film with R-BINOL and ca. half the coverage shows the same characteristics, see Figure S7. As expected the initial extinction and CD is cut in half but the same PRE effect at 340 nm and circular differential scattering develop along with the structural change of the film. Thus, the effects can be observed in a wider thickness range.

A measurement artifact as the potential origin for the presented phenomena can be excluded because of the following reasons. The extinction and CD spectrum of the pristine BK7 substrate show now specific transitions or spectral features, see Figure S8. Particularly, the CD is zero for all wavelengths and both propagation directions of the light. An influence from the substrate or substrate holder can therefore be excluded. From an instrumental standpoint, the measured extinction and CD values are within the specifications of the manufacturer. A coverage series was carried out in order to prove this experimentally and to rule out anomalous behavior at higher coverage and extinction. As expected, the measured extinction and CD depend linearly on the coverage and film thickness throughout the whole range and especially no deviation from this relation is seen for high coverages, see Figure S9. Further, no curves show signs of saturation, e.g. flattening or an increased noise level. Finally, similar behavior has been seen on films of different molecules measured with a different CD-spectrometer before.<sup>[15]</sup>

## 2.2. Structural Analysis and Nonlinear Optical Activity

Because the phase transition within the film correlates with both PRE effects the question about the structure rises.

The white spots in the film which were seen 6 h after the evaporation reveal to be circular shaped domains with a diameter of ca. 400  $\mu\text{m}$  (see Figure 5a) if investigated under the microscope with 50 $\times$  magnification (3 h after the evaporation). A black spot is visible in the center of the domain. This was likely a dust particle which could function as seed from where the restructuring began. Raman spectra in a range between 200  $\text{cm}^{-1}$  and 1100  $\text{cm}^{-1}$  were obtained inside the domain and outside the domain (which is indicated by the crosses) and compared to each other and crystalline powder. It has been shown that the intensity ratios of pairs of bands at 460, 520 and 1025  $\text{cm}^{-1}$  are sensitive to the crystal structure.<sup>[12]</sup> Therefore, these regions are separately graphed in Figure 5c,d. The intensity ratio of the band pair at 1025  $\text{cm}^{-1}$  is different for the transparent film outside and inside the domain. This provides further evidence of a structural change inside the film. Compared to the crystalline powder, which presents the chiral, crystalline form of R-BINOL, the intensity ratio for the bands within the domain matches well. This is not clearly the case for the band pairs at 460  $\text{cm}^{-1}$  and 520  $\text{cm}^{-1}$ . However, the Raman spectrum of the domain shows more similarities with the one of the crystalline form than the transparent, initial structure. This



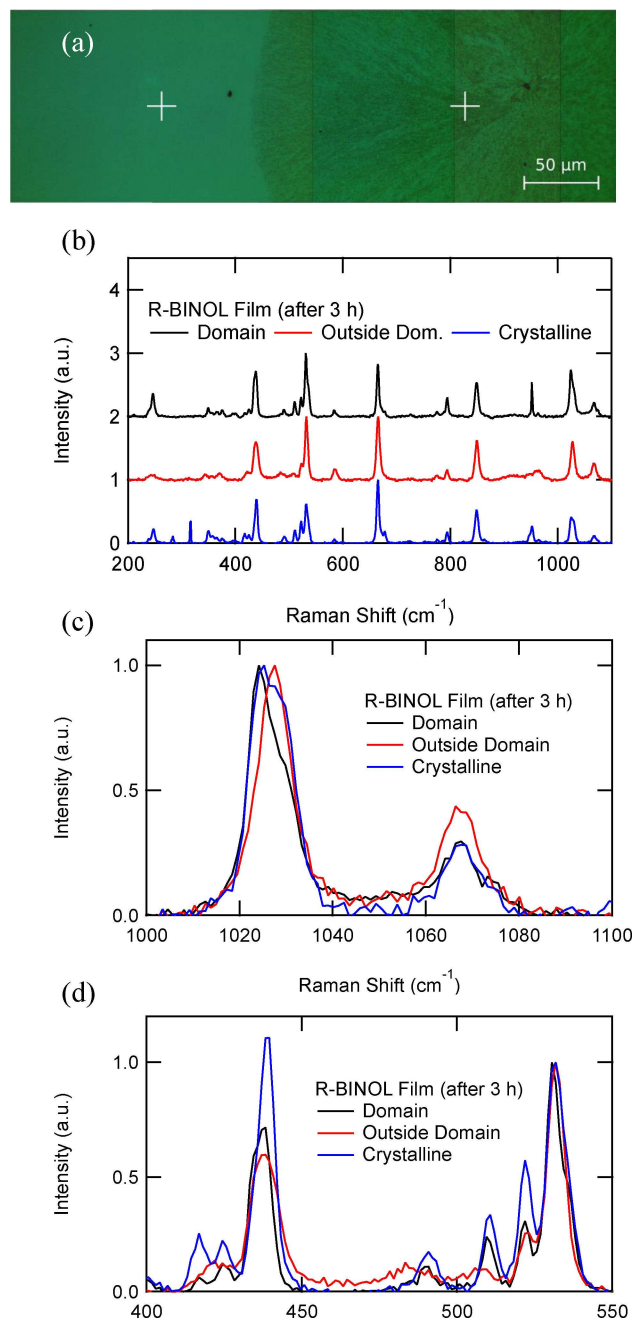


**Figure 5.** (a) Microscope picture of R-BINOL film 3 h after evaporation. Crosses indicate the positions where Raman spectra were obtained inside and outside the circular domain. (b) Raman spectra of the film and crystalline powder and normalized parts of the spectra are shown in (c) and (d). The excitation wavelength was 633 nm.

indicates that the structure of the film is getting closer to the crystalline, chiral form during the process of the restructuring.

A similarly prepared R-BINOL film on a silicon wafer was investigated with a microscope under cross polarization (Figure 6a,b) and dark field conditions (Figure 6c). Under cross polarization the film shows domains of about 1 mm in diameter. All domains show dark crosses (isogyres), which are similarly aligned as a consequence of the cross polarization. Since the

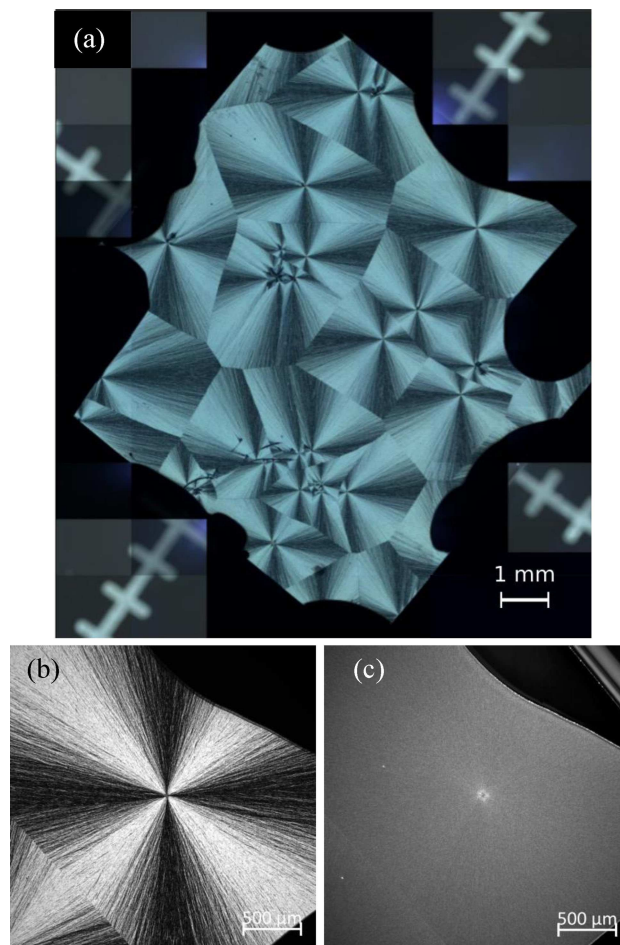


**Figure 6.** (a) Cross polarization picture of a R-BINOL film and zoom into top right part (b) and dark field picture of the zoom (c).

microscope was working with visible light this is direct proof of polarization effect in this wavelength range and the relation to the evolved structure. As reference, the picture shows dark shadows in the corners and edges of the sample, which come from the pure substrate (shadow of the clamp during evaporation) and glue and look dark since they are not optically active. The domain structure appears similar to a pseudo-focal conic phase, which is known from liquid crystals<sup>[17]</sup> where BINOL derivatives are also used as chiral dopant.<sup>[18]</sup> Figure 6b shows a zoom on the top right domain. Besides the isogyres, fine radial lines beginning from one center point can be seen. When switched to dark field a bright spot is visible where the melatope (crossing of the isogyres) in the cross polarization picture lies. Because this finding is exemplary for all other domains, it confirms the hypothesis that the phase transition is seeded from imperfections.

SHG-CD measurements were performed on this sample to gain further knowledge about the optical activity and orientation of the molecules<sup>[19]</sup> within a domain, since the two are connected in the nonlinear regime. A circularly polarized laser beam, with a wavelength of 800 nm, was focused onto the sample while the sample was rotated around the surface

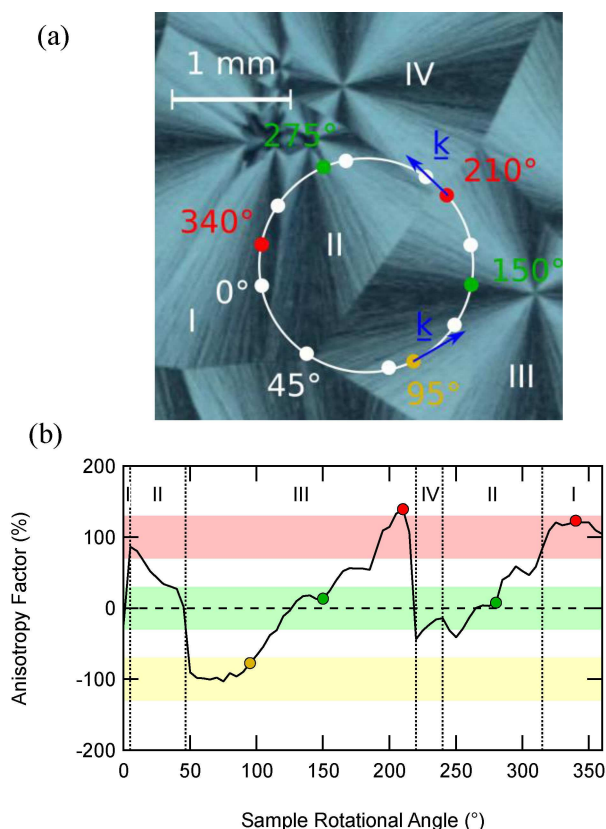


**Figure 7.** (a) Cross polarization picture of a R-BINOL film with the laser beam path during anisotropy factor measurements while the sample rotates around surface normal. (b) Related second order anisotropy factor at 400 nm SH for R-BINOL film at according sample rotational angle.

normal. The laser path is depicted in Figure 7a and crosses several domains in the center (see Figure 6a). The propagation vector  $\underline{k}$  of the light is shown as an arrow for several angles. As the sample is rotated the intensity of the SH at 400 nm (in the scattering region and beyond the low energy absorption band) is detected. The difference between the SH intensities  $I_{\text{LCP/RCP}}$  generated by the left circularly polarized (LCP) and right circularly polarized (RCP) fundamental light is weighted by the average resulting in the commonly defined second order anisotropy factor<sup>[20]</sup>

$$g = \frac{I_{\text{LCP}} - I_{\text{RCP}}}{1/2 (I_{\text{LCP}} + I_{\text{RCP}})}$$

This anisotropy factor is plotted against the sample rotation angle in Figure 7b.

As one can see the anisotropy factor varies strongly with the sample orientation and, therefore, the position of the laser spot on the sample. If concentrating on the path inside domain III between 50° and 220° the anisotropy factor increases from roughly -100% to 100%. At 100° the propagation vector  $\underline{k}$  is parallel to the radial lines pointing to the center spot in the cross-polarization picture whereas at 210° it is pointing away. The anisotropy factor is about the same in absolute at the two

angles but show the opposite sign. In the nonlinear regime, the optical activity does not only depend on the activity of individual molecules but also on their orientation and long-range order in the sample. Thus, the anisotropy factor can reveal information about the average orientation of the molecules at the laser spot.<sup>[19]</sup> It follows that on average the molecules are orientated opposite to the propagation vector at the two mentioned sample angles. This is the case, if for example, the molecules are aligned in chains, which are spreading in a radial matter from the center point of each domain. Finally, a structure of focal conic domains in smectic films is proposed based on the available knowledge.<sup>[21,22]</sup>

If the domain size gets smaller than the laser spot size, the recorded anisotropy factor would be an average of multiple domains as in case of the linear CD studies. An S-BINOL film with domain sizes smaller than the laser spot (see Figure S10a) was investigated. The anisotropy factor was constant at a value of -26(2)%, independent of the sample rotation angle (Figure S10b).

### 2.3. Theoretical Description

So far, the optical activity is assumed to originate from pure circular dichroism. However, other effects such as linear birefringence (LB) and linear dichroism (LD) cannot be ruled out yet. Both are based on the interaction of linearly polarized light with the sample and a difference between polarizations perpendicular to each other. The superposition of CD, LD and LB can be derived for a general sample using the Mueller matrix approach.<sup>[23]</sup> The signal of the CD spectrometer is expressed as

$$S = A [CD + 1/2 (LD' LB - LD LB')] + B [LB' \sin(2\theta) - LB \cos(2\theta)]$$

where  $A$  and  $B$  are apparatus constants, which are described in detail in the SI.  $LD$  is linear dichroism and  $LD'$  is linear dichroism for a sample rotated at 45° around the surface normal.  $\theta$  is the rotational angle of the sample around the surface normal.<sup>[24]</sup> It follows that contributions from  $LB$  and  $LB'$  can be isolated by comparing signals at different sample angles. This has been done with one S-BINOL film in both propagation directions and the results are plotted in Figure 8. Neither the extinction nor the optical activity alters significantly under rotation, but they are affected by flipping the sample. Thus, the second term including  $LB$  and  $LB'$  is negligible or zero. To show that the apparatus dependent factor  $B$  is nonzero, a baseline without sample was acquired. As shown in Figure S11, the baseline is nonzero and changes with wavelength. Therefore, it is concluded that  $LB$  and  $LB'$  are negligible or zero.

Furthermore, the difference in optical activity between opposite propagation direction of the light can be expressed as:<sup>[23]</sup>

$$\Delta S = A (LD' LB - LB' LD) + 2 B LB' \sin(2\theta)$$

with transformations  $LB = LB$  and  $LB' = -LB'$  (analog for  $LD$ ).

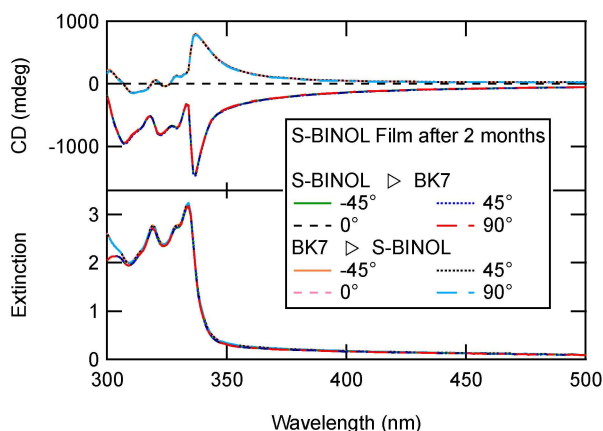


**Figure 8.** Extinction and CD of S-BINOL film for different rotational angles around the surface normal 2 months after evaporation. Note that curves of same propagation direction overlay.

Thus, the model predicts that the reversal of ellipticity is caused by a combination of LB and LD. Note that contributions from CD are subtracted out here. The latter term is only dependent on  $LB'$  and therefore neglected. The PRE is then defined as the product of LB and LD.

There are two possible interpretations. First, LD is the dominant effect present. Even multiplied with negligible contributions from LB it is strong enough to explain the observed PRE. The latter is rather unlikely as the radial symmetry of each domain by definition cannot cause LB and LD. Thus, this holds even if the applied theoretical model is incorrect. In case of LB, this is experimentally proven and unlikely to be different for LD. The second interpretation is that the model is simply inadequate or incomplete. For example, the model does not consider domain boundaries and interfaces between neighboring domains. In addition, the three dimensionality of the sample is ignored.

For the sake of completeness, several important studies should be discussed regarding their relevance for the interpretation of the observations in this work. A vibrational CD (VCD) study on solid polymer films and effects of the sample orientation by Merten *et al.* should be mentioned.<sup>[25]</sup> In this work, films of achiral polymers were rotated around the surface normal and flipped with respect to the propagation direction of the light in a similar manner as done here. The VCD signal shifted strongly upon sample rotation, and even led to opposite signs of the recorded VCD. Whereas, sample flipping led to inversion of 'artificial' VCD bands, which was also seen in another study from Buffeteau *et al.* by again simple rotation of the sample.<sup>[26]</sup> A theoretical description of the effects based on the Mueller matrix approach was also provided. However, there are important differences between these findings and the effects observed here. First, in comparison to the works of Merten and Buffeteau, the CD of the BINOL film does not change with sample rotation. Second, the CD feature showing PRE is unambiguously related to transitions of BINOL and are not of artificial nature. Third, the proposed formalism in these

works cannot explain the enantiosensitivity of the effect observed in the present work. Another work, which should be mentioned at this point is the microscopy study on chiroptical artifacts by the group of Bart Kahr. The team demonstrated how LB causes artificial "CB" and "CD" signals in thick polycrystalline spherulites of D-sorbitol and developed a theoretical description.<sup>[27]</sup> Interestingly, the formalism considers several key properties of the system studied here like e.g. the rotational symmetry of a single domain, the three-dimensional character of the film and the interface between neighboring domains. However, the experimental and theoretical findings are described on a local level. The LB, as it is proposed to be generated at interfaces between neighboring domains would average to zero, upon averaging over a large number of domains, as it is the case in our work. Also, the proposed formalism would ignore the correlation between the PRE effect in the CD signal and transitions of BINOL. Equally importantly, it cannot explain the enantiosensitivity of this effect as already correctly stated by the same group.<sup>[28]</sup>

Summarizing it is proposed that the observed PRE cannot be explained by LB and LD in connection with the standard model and it is indeed an effect of CD, which is not considered in this model.

Note that the spectra in Figure 8 were taken 2 months after the evaporation and are identical to the spectra shown previously. The samples were stored in air and at room temperature. Thus, once the film changes into the crystalline phase it stays stable over an extended period of time.

### 3. Conclusion

In conclusion, BINOL films with a thickness of 1.5  $\mu\text{m}$  were prepared by evaporation. The initial transparent films showed an additional negative cotton effect at 337 nm the wavelength of the low energy absorption band compared to the solution phase. 6 h after the evaporation the sample showed circular shaped white domains which was assigned as the beginning of a structural phase transformation within the film. At this stage the CD spectrum showed an additional cotton effect at 340 nm which showed PRE when the sample was flipped with respect to the light path as well as with change of the enantiomer. This PRE was related to dipole-dipole interactions between neighboring molecules in the new structural phase. Raman spectroscopy confirmed this structural change and showed similarities between the crystalline, chiral form of BINOL and the final film structure. The phase transition at room temperature was finished after 3 d and the sample showed a white appearance, which was proven as Rayleigh scattering beyond the absorption of BINOL throughout the visible range and showed optical activity. The circular differential scattering underwent PRE when the sample was flipped but not with change of the enantiomer in contrast to the previous mentioned effect in the absorption region. This underlined that both effects showing PRE are of fundamentally different origin.

A combined study of microscopy under cross polarization settings and SHG-CD revealed the structure and orientation of

the molecules and a structure of focal conic domains with radial symmetry in smectic film is proposed. Furthermore, the SHG-CD experiments showed that the films are also optically active in the nonlinear regime.

A theoretical description through the Mueller matrix approach and comparison to the results was made. It is argued that the effects LB and LD are negligible and that the enantioselective PRE is caused by CD but indescribable with the standard model.

Compared to systems which showed PRE the one presented here does not possess a double-layer meta-interface nor an enantiomerically sensitive plasmon and is simpler in sense of preparation and material composition. We believe therefore that PRE is not limited to such systems.

In summary, CD of solid-state samples with isotropy are more complicated than in solution. Due to the superposition of the optical activity of individual molecules and effects caused by long-range order the interpretation is more challenging. However, vice versa if a sufficient model can be found, describing all contributions, additional structural information can be derived from CD measurements.

## Acknowledgements

This work has been supported by the DFG through the project (HE 3454/21-1) and through the projects Alberta/Technische Universität München Graduate School for Functional Hybrid Materials ATUMS (IRTG2022). VKV acknowledges support from the Royal Society through the University Research Fellowships and through Grant Nos. CHG\R1\170067, PEF1\170015, and RGF\EA\180228, as well as from the STFC Grant No. ST/R005842/1. DCH acknowledges funding and support from the Engineering and Physical Sciences Research Council (EPSRC) Centre for Doctoral Training in Condensed Matter Physics (CDTCMP), Grant No. EP/L015544/1.

## Conflict of Interest

The authors declare no conflict of interest.

**Keywords:** circular dichroism • ellipticity • films • isotropy • second-harmonic generation

- [1] N. Berova, K. Nakanishi, R. Woody, *Circular Dichroism: Principles and Applications*, Wiley, 2000.
- [2] V. A. Fedotov, A. S. Schwanecke, N. I. Zheludev, V. V. Khardikov, S. L. Prosvirnin, *Nano Lett.* **2007**, 7, 1996–1999.
- [3] S. Tomita, Y. Kosaka, H. Yanagi, K. Sawada, *Phys. Rev. B – Condens. Matter Mater. Phys.* **2013**, 87, 041404.
- [4] Q. L. Zhou, *Privileged Chiral Ligands and Catalysts*, 2011.
- [5] J. M. Brunel, *Chem. Rev.* **2007**, 107, PR1–PR45.
- [6] P. Heister, T. Lunsken, M. Thamer, A. Kartouzian, S. Gerlach, T. Verbiest, U. Heiz, *Phys. Chem. Chem. Phys.* **2014**, 16, 7299–7306.
- [7] D. C. Hooper, A. G. Mark, C. Kuppe, J. T. Collins, P. Fischer, V. K. Valev, *Adv. Mater.* **2017**, 29, 1605110.
- [8] Y. R. Shen, *Fundamentals of Sum-Frequency Spectroscopy*, Cambridge University Press, 2016.
- [9] S. H. Han, N. Ji, M. A. Belkin, Y. R. Shen, *Phys. Rev. B* **2002**, 66, 165415.
- [10] B. Suchod, A. Renault, J. Lajzerowicz, G. P. Spada, *J. Chem. Soc. Perkin Trans. 2* **1992**, 1839–1844.
- [11] S. F. Mason, *Molecular Optical Activity and the Chiral Discriminations*, Cambridge University Press, 1982.
- [12] A. R. Lacey, F. J. Craven, *Chem. Phys. Lett.* **1986**, 126, 588–592.
- [13] K. A. Kerr, J. M. Robertson, *J. Chem. Soc. B* **1969**, 1146–1149.
- [14] R. B. Kress, E. N. Duesler, M. C. Etter, I. C. Paul, D. Y. Curtin, *J. Am. Chem. Soc.* **1980**, 102, 7709–7714.
- [15] G. Lakhwani, S. C. J. Meskers, R. A. J. Janssen, *J. Phys. Chem. B* **2007**, 111, 5124–5131.
- [16] C. Bustamante, I. Tinoco, M. F. Maestre, *Proc. Natl. Acad. Sci. USA* **1983**, 80, 3568–3572.
- [17] T. Frizon, Dal-Bó, Lopez, D. Silva Paula, D. Silva, *Liq. Cryst.* **2014**, 41, 1162–1172.
- [18] H. Goto, K. Akagi, *Macromolecules* **2005**, 38, 1091–1098.
- [19] J. D. Byers, H. I. Yee, T. Petralli-Mallow, J. M. Hicks, *Phys. Rev. B* **1994**, 49, 14643–14647.
- [20] T. Petralli-Mallow, T. M. Wong, J. D. Byers, H. I. Yee, J. M. Hicks, *J. Phys. Chem.* **1993**, 97, 1383–1388.
- [21] W. Guo, C. Bahr, *Phys. Rev. E* **2009**, 79, 61701.
- [22] V. Designolle, S. Herminghaus, T. Pfohl, C. Bahr, *Langmuir* **2006**, 22, 363–368.
- [23] Y. Shindo, *Opt. Eng.* **1995**, 34, 3369–3384.
- [24] R. Kuroda, T. Harada, Y. Shindo, *Rev. Sci. Instrum.* **2001**, 72, 3802–3810.
- [25] C. Merten, T. Kowalik, A. Hartwig, *Appl. Spectrosc.* **2008**, 62, 901–905.
- [26] T. Buffeteau, F. Lagugné-Labarthe, C. Sourisseau, *Appl. Spectrosc.* **2005**, 59, 732–745.
- [27] J. H. Freudenthal, E. Hollis, B. Kahr, *Chirality* **2010**, 21, E20–E27.
- [28] H.-M. Ye, J. Xu, J. Freudenthal, B. Kahr, *J. Am. Chem. Soc.* **2011**, 133, 13848–13851.

Manuscript received: October 11, 2018

Revised manuscript received: November 15, 2018

Accepted manuscript online: November 16, 2018

Version of record online: December 4, 2018